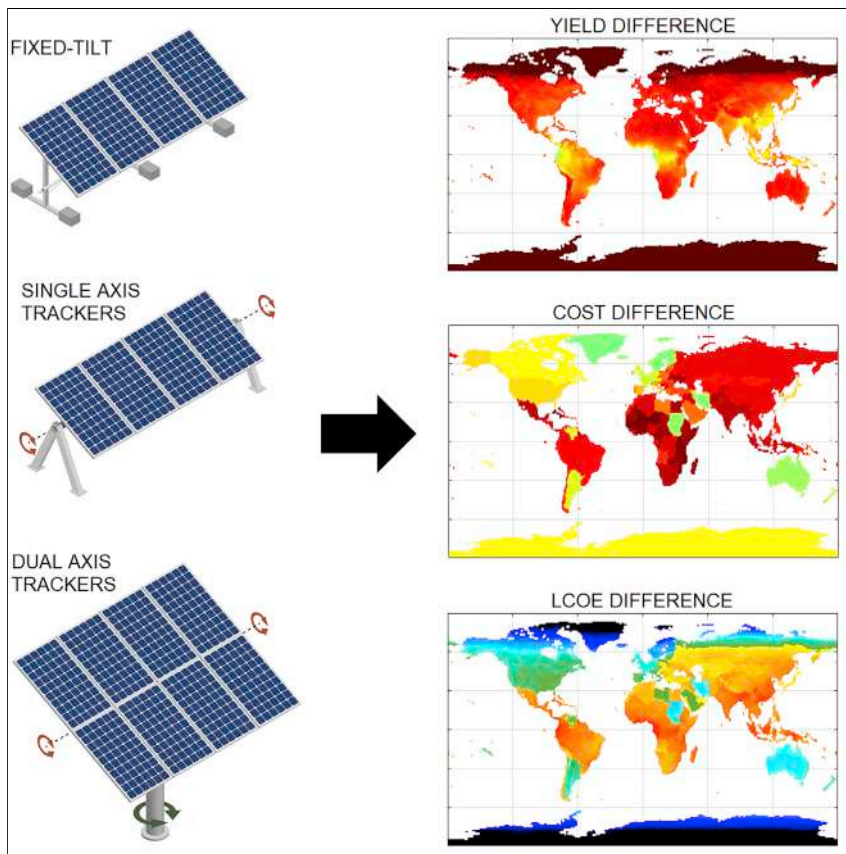


Article

Global Techno-Economic Performance of Bifacial and Tracking Photovoltaic Systems



This work performs a comprehensive techno-economic analysis worldwide for photovoltaic systems using a combination of bifacial modules and single- and dual-axis trackers. We find that single-axis trackers with bifacial modules achieve the lowest LCOE in the majority of locations (16% reduction on average). Yield is boosted by 35% by using bifacial modules with single-axis trackers and by 40% in combination with dual-axis trackers.

Carlos D. Rodríguez-Gallegos, Haohui Liu, Oktoviano Gandhi, ..., Li Li, Thomas Reindl, Ian Marius Peters

carlos.rodriguez@nus.edu.sg

HIGHLIGHTS

Techno-economic comparison of combinations of bifacial and tracking PV systems

Worldwide assessment of yield and LCOE

Bifacial modules with single-axis trackers achieve lowest LCOE in most locations

Bifacial modules with single- and dual-axis trackers boost yield by 35% and 40%

Article

Global Techno-Economic Performance of Bifacial and Tracking Photovoltaic Systems

Carlos D. Rodríguez-Gallegos,^{1,7,*} Haohui Liu,¹ Oktoviano Gandhi,¹ Jai Prakash Singh,¹ Vijay Krishnamurthy,¹ Abhishek Kumar,¹ Joshua S. Stein,² Shitao Wang,³ Li Li,⁴ Thomas Reindl,¹ and Ian Marius Peters^{5,6}

SUMMARY

This work presents a worldwide analysis on the yield potential and cost effectiveness of photovoltaic farms composed of monofacial fixed-tilt and single/dual (1T/2T) tracker installations, as well as their bifacial counterparts. Our approach starts by estimating the irradiance reaching both the front and rear surfaces of the modules for the different system designs (validated based on data from real photovoltaic systems and results from the literature) to estimate their energy production. Subsequently, the overall system cost during their 25-year lifetime is factored in, and the levelized cost of electricity (LCOE) is obtained. The results reveal that bifacial-1T installations increase energy yield by 35% and reach the lowest LCOE for the majority of the world (93.1% of the land area). Although dual-axis trackers achieve the highest energy generation, their costs are still too high and are therefore not as cost effective. Sensitivity analyses are also provided to show the general robustness of our findings.

INTRODUCTION

Solar photovoltaic (PV) systems have become a major contributor to global electricity generation with more than 600 GWp of accumulated installed capacity as of 2019.¹ In many regions of the world, PV electricity is now cheaper than electricity from conventional sources like coal, making PV, together with wind, the most commonly installed new generation source.² The majority of current PV installations employ monofacial crystalline silicon PV modules^{3,4} with a fixed-tilt system setup. Yet, the emergence of two technologies at cost-competitive levels is likely going to disrupt this dominance: (1) bifacial modules are able to collect light not only from the front, but also from the rear. (2) single (1T)- and dual (2T)-axis tracking systems adjust the module orientation to follow the sun's position. Both technologies significantly enhance the energy yield of a PV system and have the potential to be combined (i.e., bifacial tracking) to further improve performance. Previously, these technologies required considerably higher up-front investment costs, which discouraged potential investors. However, bifacial modules and tracking systems have experienced a progressive decrease in cost in recent years^{5–9} to such a degree that their revenue advantages due to increased energy production are now outweighing the higher system cost. The aim of this study is to analyze the location-specific operating conditions, including climatic and economic factors, and to establish which combinations of bifacial and tracking systems are economically favorable.

Context & Scale

Energy production of photovoltaic (PV) modules can be increased not only by solar cells that are more efficient but also by innovative system concepts. In this study, we explore two such concepts in combination: tracking and bifacial modules. A tracking setup increases energy production by moving a PV module over the course of a day, so that it always faces the sun. Bifacial modules use special solar cells and a transparent cover to collect light not only from the front but also from the rear. Through recent advances, both concepts have seen price reductions that enable them to produce electricity cheaper than conventional PV systems. Here, we analyze the technical and economic aspects of combinations of these two concepts worldwide. We find that a combination of bifacial modules with one-axis trackers produces the cheapest electricity (LCOE 16% lower than conventional systems) by significantly boosting energy production (35% more than conventional systems).

A variety of studies have aimed to predict the energy gain (G) of bifacial and tracking designs in specific locations around the world. A summary of the findings is presented in [Table 1](#). It is important to notice that many of these results correspond to the gain from single-module systems (as indicated in the second row from this table). These will not be representative of gains expected for larger systems.

Worldwide analyses have also been carried out to study the advantages of bifacial modules over monofacial ones for fixed-tilt systems.^{27–30} These previous studies show that the system-specific increase in module elevation from ground and high albedo values are particularly effective in enhancing energy generation from bifacial modules. Moreover, bifacial modules were found to generate greater gains at locations with high latitude.

With respect to studies on tracking systems worldwide, Jacobson et al.³¹ compared the irradiance collection from monofacial 1T and 2T systems with respect to the global horizontal irradiance for locations at sea and land. In addition, Pelaez et al.²¹ analyzed the gain on the irradiance collection from bifacial-1T designs with respect to their monofacial counterparts for many locations worldwide.

While improvements in the energy yield of bifacial and tracking systems have been studied in great detail, their ability to lower LCOE globally is less understood. LCOE is of particular interest as it is the key to determine the return on investments for PV installation companies and investors. A question yet to be answered is whether the extra energy produced from bifacial and tracking systems are able to overcome their extra cost; i.e., will these systems have a lower LCOE than standard monofacial fixed-tilt installations?

Hence, in this paper, we explore the cost effectiveness of monofacial and bifacial PV farms with fixed-tilt, 1T and 2T installations worldwide. A sketch of the analyzed mounting structures is presented in [Figure 1](#), also indicating the irradiance reaching both the front and rear sides. As the first step, we developed a performance model for the different mounting approaches using satellite data ([Methodology](#)). We calibrated this model against field-measured data from fixed-tilt and tracking installations and showed agreement with an overall deviation below 3% ([Validation of Irradiance Calculation Methodology](#)). We then extended this study globally, based on the parameters provided in [Global Techno-Economic Performance Calculation](#), and investigated the technical and economic performance of the different mounting configurations ([Results](#)). Finally, we explored the sensitivity of LCOE in a variety of locations using a Monte Carlo and region sensitivity approach ([Results](#)). This analysis shows what changes in LCOE should be expected for variations related to weather, module, and cost parameters. A general discussion on the previous results is presented in [Discussion](#), and the paper is concluded in [Conclusions](#).

Methodology

Calculation of Global/Diffuse Horizontal and Direct Normal Irradiance

Daily average (one value per day) global horizontal irradiance (GHI) is obtained from NASA's Clouds and the Earth's Radiant Energy System (CERES).³² Due to the influence of the sun's position on the overall irradiance collected at the module surface, it is necessary to estimate the irradiance values with a higher resolution. This is achieved by employing an approach similar to the one presented in Sun et al.²⁹ The hourly GHI is first estimated by applying the clear sky model proposed by Haurwitz.^{33,34} In an effort to reduce estimation errors, the hourly GHI values are multiplied by a constant so that their average is equal to the daily average GHI provided by

¹Solar Energy Research Institute of Singapore (SERIS), National University of Singapore (NUS), Singapore 117574, Singapore

²Sandia National Laboratories, Albuquerque, NM 87185, USA

³Harbin Institute of Technology, School of Astronautics, Harbin 150001, China

⁴Harbin Institute of Technology, School of New Energy, Weihai 264209, China

⁵MIT Photovoltaic Research Laboratory (PV-Lab), Massachusetts Institute of Technology (MIT), Cambridge, MA 02139, USA

⁶Present address: Helmholtz Institute Erlangen-Nürnberg for Renewable Energy, 91058 Erlangen, Germany

⁷Lead Contact

*Correspondence: carlos.rodriguez@nus.edu.sg
<https://doi.org/10.1016/j.joule.2020.05.005>

Table 1. Literature Review on the Energy Gain of Different Designs

Location	Module Elevation (m)/ Number of Modules Forming the System	Albedo/Bifaciality	Tilt(°)/Facing	G (%)	Comments
Amsterdam, The Netherlands ^{a,10}	0.5/1	0.2(0.5)/0.923	90/east	10.4(29.5)	monofacial module: optimum tilt angle/south
Doha, Qatar ^{a,10}	0.5/1	0.2(0.5)/0.923	90/east	-5.6(17.2)	
Amsterdam, The Netherlands ^{a,11}	?/7 rows	0.3/0.8	optimum orientation for fixed-tilt systems	>5 and <12	N/A
	?/7 rows	0.3/0.8		>6 and <15	monofacial-1T versus monofacial fixed-tilt
	?/7 rows	0.3/0.8		>10 and <26	bifacial-1T versus monofacial fixed-tilt
Doha, Qatar ^{a,11}	?/7 rows	0.3/0.8	optimum tilt angle for fixed-tilt systems	>4 and <10	N/A
	?/7 rows	0.3/0.8		>8 and <20	monofacial-1T versus monofacial fixed-tilt
	?/7 rows	0.3/0.8		>12 and <29	bifacial-1T versus monofacial fixed-tilt
Thuwal, Saudi Arabia ^{b,12}	0.2/1	gray gravel/?	25(45)/south	~13.5(~14.8)	N/A
Winterthur, Switzerland ^{a,13}	0.5(2)/35	0.51/0.85	30/south	~15.3(~16.5)	gain calculated from only 1-day data: 15 October 2017
Oslo, Norway ^{a,14}	1/1	0/0.8	?/south	~6.0	monofacial module: standard orientation
	1/1	0.2/0.8	~51.0/south	~10.3	
	1/1	0.5/0.8	~46.0/south	~16.4	
Cairo, Egypt ^{a,14}	0.5/1	0/0.8	?/south	~1.4	
	0.5/1	0.2/0.8	~26.9/south	~11.0	
	0.5/1	0.5/0.8	~24.9/south	~24.7	
El Gouna, Egypt ^{a,15}	1.5/1	0.2(0.5)/?	25/south	13.46(33.85)	N/A
	0.5/1	0.2(0.5)/0.914	90/east	-14.88(-5.99)	monofacial module: 25°/south
Kasese, Uganda ^{a,15}	?/1	0.2(0.5)/?	?/?	16.47(43.77)	N/A
	?/1	0.2(0.5)/?	?/?	14.71(17.93)	monofacial-1T versus monofacial fixed-tilt
	?/1	0.2(0.5)/?	?/?	1.53(21.93)	bifacial fixed-tilt versus monofacial-1T
	?/1	0.2(0.5)/?	?/?	40.1(62.2)	bifacial-1T versus monofacial fixed-tilt
Konstanz, Germany ^{a,15}	1.5/1	0.2(0.5)/?	37/south	15.98(35.73)	N/A
	0.5/1	0.2(0.5)/0.914	90/east	-4.52(15.77)	monofacial module: 37°/south
Berlin, Germany ^{b,15}	1.2/2	0.3/0.914	20/south	20.53	N/A
Hamelin, Germany ^{a,16}	0.1(1)/1	~0.71/1	35/south	25(35)	N/A
	0.1(1)/1	~0.25/1	35/south	11(13)	N/A
Albuquerque, USA ^{a,17}	0.2(3)/1	0.21/0.9	5/south	8.9(17.7)	gain calculated from the average of 3-day results: clear days around summer solstice, fall equinox, and winter solstice
	0.2(3)/1	0.43/0.9	5/south	18.2(35.4)	
	0.2(3)/1	0.21/0.9	35/south	10.2(15.5)	
	0.2(3)/1	0.43/0.9	35/south	19.2(29.3)	
	0.2(3)/1	0.21/0.9	65/south	15.8(19.1)	
	0.2(3)/1	0.43/0.9	65/south	24.9(30.6)	

(Continued on next page)

Table 1. Continued

Location	Module Elevation (m)/ Number of Modules Forming the System	Albedo/Bifaciality	Tilt(°)/Facing	G (%)	Comments
Albuquerque, USA ^{b,18,19}	1.06/8	~0.55/0.9	15/south	32.5	N/A
	1.06/8	~0.55/0.9	15/west	39	N/A
	1.06/8	~0.25/0.9	30/south	19	N/A
	0.86/4	~0.25/0.9	90/south	30.5	N/A
	0.86/4	~0.25/0.9	90/west	124	N/A
	1.6/24	~0.25/0.9	N/A	~10	bifacial-1T versus monofacial-1T
Vermont, USA ^{b,20}	3.4/20	≥0.13 and ≤1/0.92	N/A	14	bifacial-2T versus monofacial-2T
	~1.5/4 for fixed-tilt 3.4/20 for 2T	≥0.13 and ≤1/0.92	30/south	41	bifacial-2T versus bifacial fixed-tilt
Oregon, USA ^{b,21}	1.5/~340	grass/0.85	N/A	7	bifacial-1T versus monofacial-1T
Richmond, VA, USA ^{a,6}	0.15/rows	0.62/0.95	≥5 and ≤40/south	>10 and <20	N/A
Golden, USA ^{b,6}	0.15(0.4)/ 3 rows	≥0.56 and ≤0.7/0.95	10/south	>5 and <10 (>5 and <25)	N/A
Davis, USA ^{b,22}	~2.5/3 rows	0.16/0.75	N/A	5	bifacial-1T versus monofacial-1T
La Higuera, Chile ^{b,23}	~2/575kWp	desert sand/~0.85	N/A	12.8	bifacial-1T versus monofacial-1T
San Felipe, Chile ^{a,24}	0.5/72	0.12(0.7)/0.85	30/north	~7(~34)	N/A
South Korea ^{b,25}	~1/6	0.06(21)/~0.82	30/south	5.25(14.47)	N/A
Hokkaido, Japan ^{b,26}	~1.5/12	grass/0.959	35/south	8.6	N/A
	~1.5/12	snow/0.959	35/south	23.0	N/A
	~1.5/12	scallop's/shells/0.959	35/south	23.3	N/A
	~1.5/12	snow/0.959	35/south	23.8	N/A
Kasese, Uganda ^{a,15}	?/1	0.2(0.5)/?	?/?	16.47(43.77)	N/A
	?/1	0.2(0.5)/?	?/?	14.71(17.93)	monofacial-1T versus monofacial fixed-tilt
	?/1	0.2(0.5)/?	?/?	1.53(21.93)	bifacial fixed-tilt versus monofacial-1T
	?/1	0.2(0.5)/?	?/?	40.1(62.2)	bifacial-1T versus monofacial fixed-tilt

Unless otherwise indicated in the column "Comments," G (gain) corresponds to the extra energy produced from a bifacial-fixed design with respect to its monofacial counterpart, both at the same orientation (indicated in the column "Tilt(°)/facing"). The symbol "?" is applied when the data of interest were not provided in the literature.

^aResults obtained from simulations.

^bResults obtained from real systems.

CERES. Consequently, this method is accurate to calculate annual total but would not be that effective for short periods. Thereafter, the direct normal irradiance (DNI) and diffuse horizontal irradiance (DHI) are estimated by employing the Orgill and Hollands model.³⁵ As the previous models require the value of the sun zenith in time, this is estimated using a solar position algorithm (SPA).³⁶

Energy Generation Modeling

Irradiance reaching the module front and rear surfaces (I_f and I_r , respectively) are obtained considering their direct, diffuse (Perez4 model³⁷), and ground (isotropic

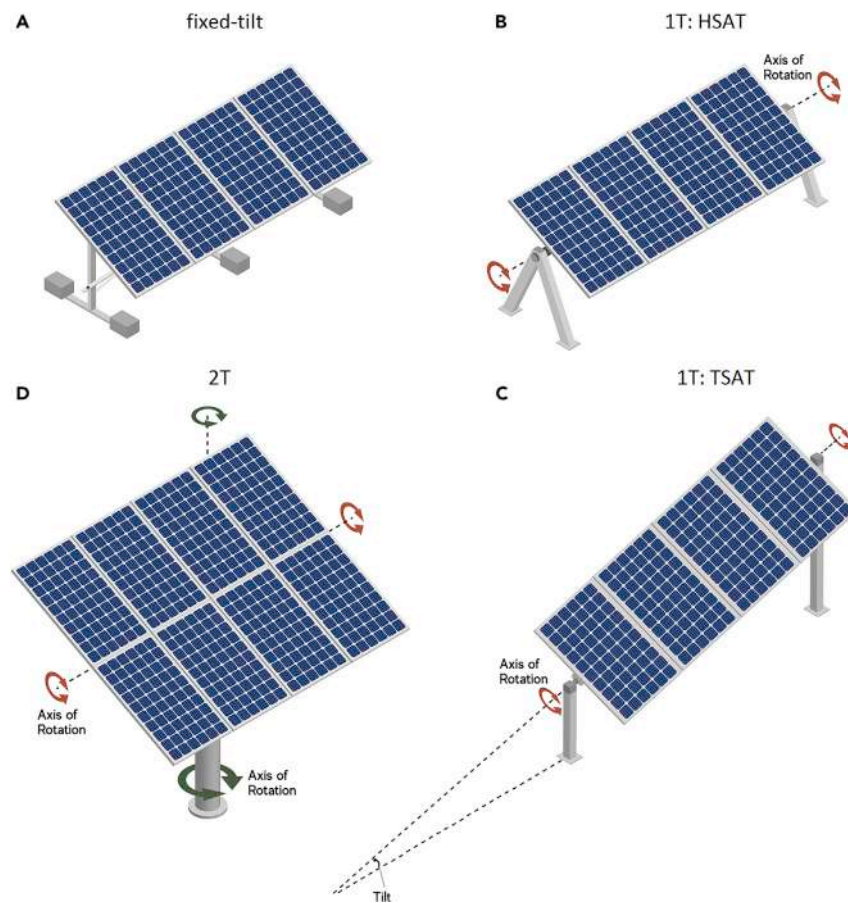


Figure 1. Sketch on the Analyzed Mounting Structures

- (A) Fixed-tilt.
- (B) Horizontal single axis tracker (HSAT).
- (C) Tilted single axis tracker (TSAT).
- (D) Dual-axis tracker.

model³⁸ and anisotropic model⁵ when calculating I_f and I_r , respectively) contributions, together with the reflection losses.^{39,40} Once I_f and I_r are obtained, the power production of a PV system can be defined as:

$$P_{PV} = \frac{P_{PV,f} \cdot (I_f + I_r \cdot b) \cdot f_1}{1000} \cdot [1 + \gamma \cdot (T_c - 25)] \cdot \eta_{inv} \cdot (1 - \beta_0 - y \cdot \beta_1) \cdot (1 - l) \quad (\text{Equation 1})$$

where $P_{PV,f}$ [W_p] is the overall power production of the installed modules under standard test conditions (STC) when light only reaches the module front side, b [%] is the bifaciality factor (equal to zero when dealing with monofacial modules), and f_1 represents the solar spectral distribution influence.^{41,42} The temperature influence on the module performance is represented by the second term from Equation 1, where γ [%/°C] is the power temperature coefficient and T_c [°C] is the cell temperature.^{43,44} The variable η_{inv} [%] represents the inverter average weighted efficiency. In addition, β_0 [%] is the initial PV degradation, while β_1 [%/year] is the yearly degradation rate (where y is the analyzed year).^{45–47} The other losses presented in a PV installation (e.g., shading, ohmic wiring losses, module mismatch, etc.) are combined and represented by the l [%] parameter.

With Equation 1, the overall energy produced by a PV system during a particular year y , $E_{PV}^{(y)}$ [Wh], can then be calculated. A detailed explanation on the power and energy estimation can be found in Rodríguez-Gallegos et al.³⁰

Estimation of the System Cost

The overall cost for the PV system during its lifetime (I_s) is defined as:

$$C_{PV} = C_{\text{Bank,int}} + C_{\text{Bank,amor}} + C_{\text{own}} + C_{\text{war}} + C_{\text{insu}} + C_{\text{OM}} \quad (\text{Equation 2})$$

where the initial investment cost, which includes the cost related to the acquisition of solar panels and inverters as well as their installation cost factor (C_{ins}), is divided into the first three terms: cost of bank interest ($C_{\text{Bank,int}}$), cost of bank amortization ($C_{\text{Bank,amor}}$), and cost of ownership (C_{own}). To cover for the initial investment of a PV farm, it is usual to obtain a bank loan to pay for part of this investment (resulting in the bank interest and amortization costs), while the owner of the PV farm is expected to pay for the rest (resulting in the cost of ownership). In addition, the inverter warranty cost (C_{war}) is incurred every few years, while insurance cost (C_{insu}) and operations and maintenance (O&M) cost (C_{OM}) of the PV farm are incurred every year. As C_{PV} corresponds to the net present value of the overall cost, the inflation and interest rates are considered when estimating the costs incurred in future years when calculating $C_{\text{Bank,int}}$, $C_{\text{Bank,amor}}$, C_{war} , C_{insu} , and C_{OM} . Further details of each of the terms can be found in Rodríguez-Gallegos et al.³⁰

Estimation of LCOE

The LCOE [USD cents/kWh], is taken as the parameter to evaluate the cost effectiveness of the analyzed PV installations. This is defined as:

$$\text{LCOE} = \frac{C_{PV}}{\sum_{y=1}^{I_s} \frac{E_{PV}^{(y)}}{(1+DR)^y}} \quad (\text{Equation 3})$$

The numerator of Equation 3 is the total cost, whereas the denominator is the energy generated by the PV system throughout its lifetime. Notice that the cost aspect of the yearly energy generation is also influenced by the discount rate, DR [%].⁴⁸

Limitations of the Presented Approach

There are several technical and economic aspects that are beyond the scope of this study. These include: No consideration of module row-row shading (and therefore, no backtracking algorithm is applied); we have assumed that the module rows were properly spaced so that these shading losses were marginal. In addition, potential shading due to the mounting structure (which includes the torque tube for trackers) and uneven irradiance at the module rear side are neglected. The influence that the row-row spacing has on other cost factors, such as site preparation works, wiring, fencing, etc., has also been neglected in this work. We do not consider governmental policies; these can have a big influence on the LCOE and therefore, determine whether it is cost effective to install a PV system in a particular location. We do not consider soiling losses in detail; soiling losses are assumed to be a part of the loss parameter l and any dependence on location or module tilt angle is not considered. We do not consider transportation costs, which are expected to have a particular influence for locations with difficult access, e.g., deserts. We also do not consider the land cost.

Most of these limitations affect the different considered system architectures in a similar way and should not affect our conclusions or performance rankings severely. If the land cost becomes significant, then the LCOE improvement from bifacial and

tracking technologies are expected to be diminished, as these technologies are likely to have a higher space requirement than the fixed-tilt ones.

Validation of Irradiance Calculation Methodology

Model validation is performed by simulating front and rear irradiance against measured values from experimental setups provided by three institutes. The measured irradiance values presented in this section were obtained from high quality sensors, which have a non-linearity accuracy below 0.3%, e.g., pyranometers Kipp and Zonen SMP10, SMP11, and CMP11.

The first analyzed data set was provided by Sandia National Laboratories and covered a time range from 17 September 2017–21 November 2017, 30 March 2018–2 May 2018, and 1 January 2019 – 9 March 2020 with a 1-min resolution for the following PV installations:

- (1) Fixed-tilt PV system: with tilt angle of 35° facing the equator, row-to-row pitch of 4.9 m, collector width of 2 m, length of the rows of 21 m and height of module lower edge of 1.1 m.
- (2) Horizontal single-axis tracker system (HSAT): with east-west rotation composed of two tracker rows (referred as HSAT 1 and HSAT 2), row-to-row pitch of 6.1 m, collector width of 2 m, length of the rows of 25 m and tracker axis height of 1.7 m.

These PV installations are located at Albuquerque, USA (latitude of 35.05° , longitude of -106.54° and elevation of 1,657 m). The data provided by Sandia National Laboratories include GHI, DNI, DHI, module orientation over time, height of rear irradiance sensors, and albedo. In addition, the sun position is estimated using the SPA algorithm introduced in [Calculation of Global/Diffuse Horizontal and Direct Normal Irradiance](#). These data are then applied to compute the irradiance reaching the front and rear sides of the modules for these PV installations. The results are then compared with the measured irradiance falling on either module plane.

[Figure 2](#) shows the time series of the simulated and measured irradiance for three selected days with specific weather conditions (sunny, partly cloudy, and cloudy). [Figure 3](#) shows the relation between the measured and simulated irradiance values for the entire period considered. In general, we find decent agreement between measurement and simulation. A larger discrepancy occurs at the module rear side with a normalized root-mean-square error (NRSME) of approx. 5%–6%. The rear irradiance only contributes a small fraction of the total irradiance. Hence, we find similar NRMSEs of approx. 2%–3% for both front and front + rear. [Figure 3](#) also provides the overall relative difference between the measured and simulated overall insolation (I_d).

In addition to validating the bifacial irradiance calculation model, the accuracy of long-term irradiance calculation using satellite data (following the approach from [Calculation of Global/Diffuse Horizontal and Direct Normal Irradiance](#)) is also validated against field measurements. Here, we used field measurement results collected by Harbin Institute of Technology (HIT) with a testbed located at Weihai, China (latitude of 37.53° , longitude of 122.08° , and elevation of ~ 10 m). More than one year of irradiance data are used. The following describe their analyzed PV systems:

- (1) Fixed-tilt PV system: with tilt angle of 34° facing the equator, row-to-row pitch of 10 m, collector width of 2 m, length of the rows of 36 m and height of module lower edge of 0.3 m. Only front side irradiance is recorded.

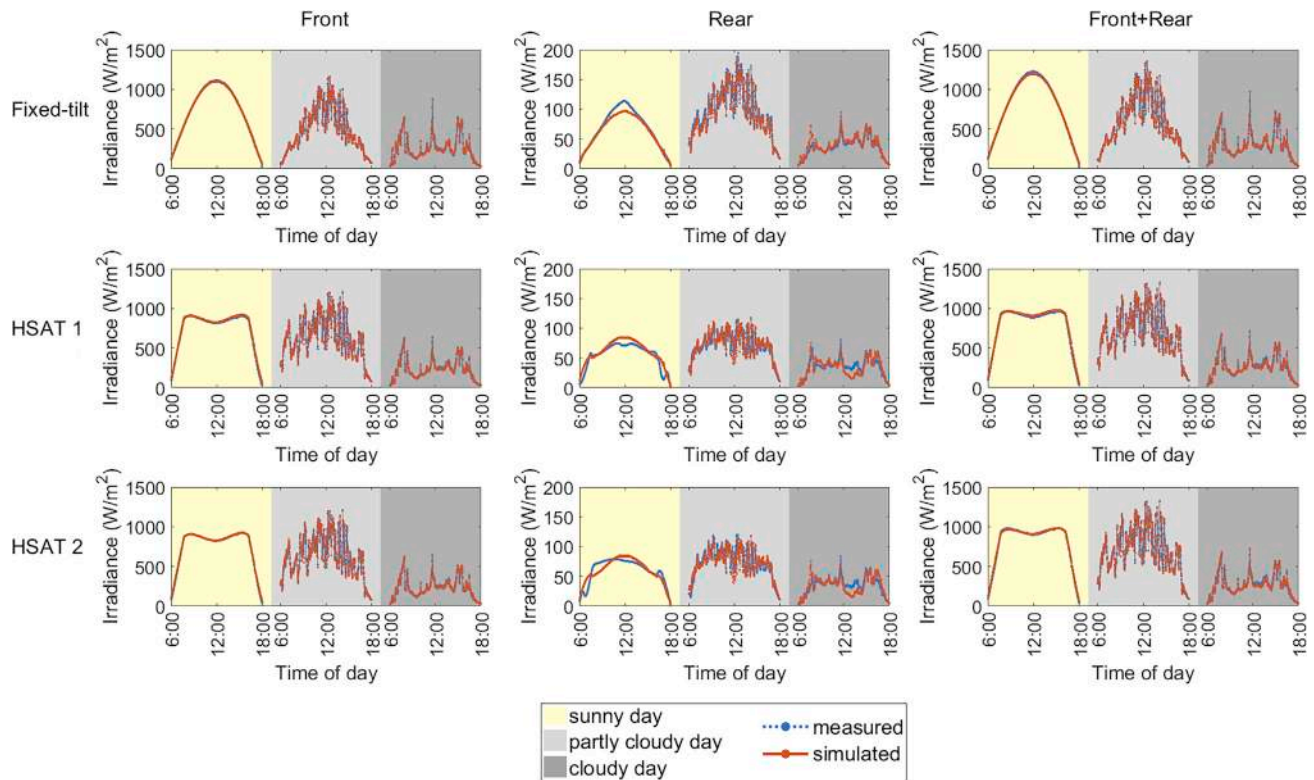


Figure 2. Time Series of Measured and Simulated Irradiance for 3 Days (Sunny, Partly Cloudy, and Cloudy) Falling at the Front, Rear, and Front and Rear Sides of the Modules for the Fixed-Tilt PV Installation and the Two Tracker Rows of the HSAT PV Installation located at United States

- (2) Tilted single-axis tracker system (TSAT): with 20° tilt and east-west rotation, row-to-row pitch of 5.6 m, collector width of 1.7 m, length of the rows of 31 m and tracker axis height of 2.4 m. Front and rear side irradiance are recorded.
- (3) HSAT: with east-west rotation, row-to-row pitch of 9.2 m, collector width of 2 m, length of the rows of 47 m and height of the tracker axis of 2.2 m. Only front side irradiance is recorded.

The monthly front and rear insolation received by the tracker systems is compared against the front side insolation of the fixed-tilt system by calculating the following ratios:

- (1) $TSAT_{f+r}/fixed_f$: Ratio between combined front and rear insolations collected by the TSAT system with respect to the front insolation of the fixed-tilt system.
- (2) $HSAT_f/fixed_f$: Ratio between front insolation collected by the HSAT system with respect to the front insolation of the fixed-tilt system.

These measurement-based results, together with their respective simulated-based ones, are presented in Figure 4 in the form of bars. In addition, markers indicate the percentage of difference between the measured and simulated results. The final bars (and markers) shown in this plot correspond to the average values from these historical data, where the average percentage of difference between the measured and simulated ratios from $TSAT_{f+r}/fixed_f$ and $HSAT_f/fixed_f$ are 1% and 5%, respectively. Here, it can be appreciated that simulation results agree very well with field measurement.

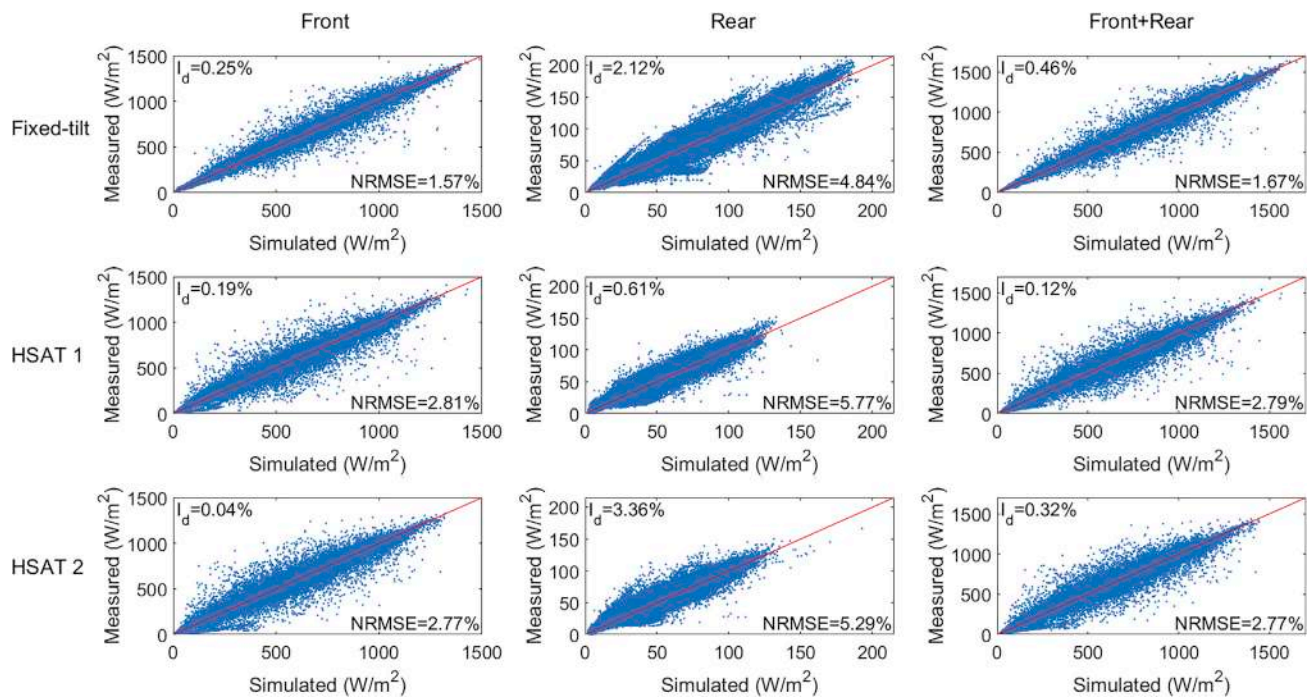


Figure 3. Measured versus Simulated Irradiance Falling at the Front, Rear, and Front and Rear Sides of the Modules for the Fixed-Tilt PV Installation and the Two Tracker Rows of the HSAT PV Installation located at USA

The red line represents the case when measured and simulated values are equal.

Model validation is also applied based on the one-minute resolution irradiance data (GHI, DHI, DNI, and front side irradiance) provided by the Solar Energy Research Institute of Singapore (SERIS) for their setups with fixed-tilt installations located at:

- (1) Singapore: latitude of 1.30° , longitude of 103.77° , elevation of ~ 36 m, and data range from 1 June 2010–14 March 2020. This setup is composed of an irradiance sensor with tilt angle of 10° and azimuth of 60° NE.
- (2) Australia: latitude of -23.76° , longitude of 133.88° , elevation of ~ 631 m and data range from 13 July 2017–14 March 2020. This PV system has a tilt angle of 24° facing the equator, row-to-row pitch of 6.5 m, collector width of 3 m, length of the rows of 21 m, and height of module lower edge of 1.7 m.
- (3) Germany: latitude of 51.77° , longitude of 11.77° , elevation of ~ 125 m, and data range from 23 December 2017–14 March 2020. This PV system has a tilt angle of 35° facing the equator, row-to-row pitch of ~ 14 m, collector width of 3 m, length of the rows of ~ 39 m, and height of module lower edge of ~ 0.5 m.

Figure 5 shows the comparison between the measured and the simulated front irradiances reaching the modules for these locations, where accurate simulation results can be appreciated once more.

Moreover, the irradiance estimation approach presented in this paper is also validated with the values found in literature. As indicated in the introduction, some research has estimated the irradiance collection for different tracking configurations worldwide. In Jacobson and Jadhav,³¹ the average ratio (considering sea and land) between the incident insolation on monofacial-1T and monofacial-2T designs with respect to the global horizontal insolation is 1.35 and 1.39, respectively. The ratio

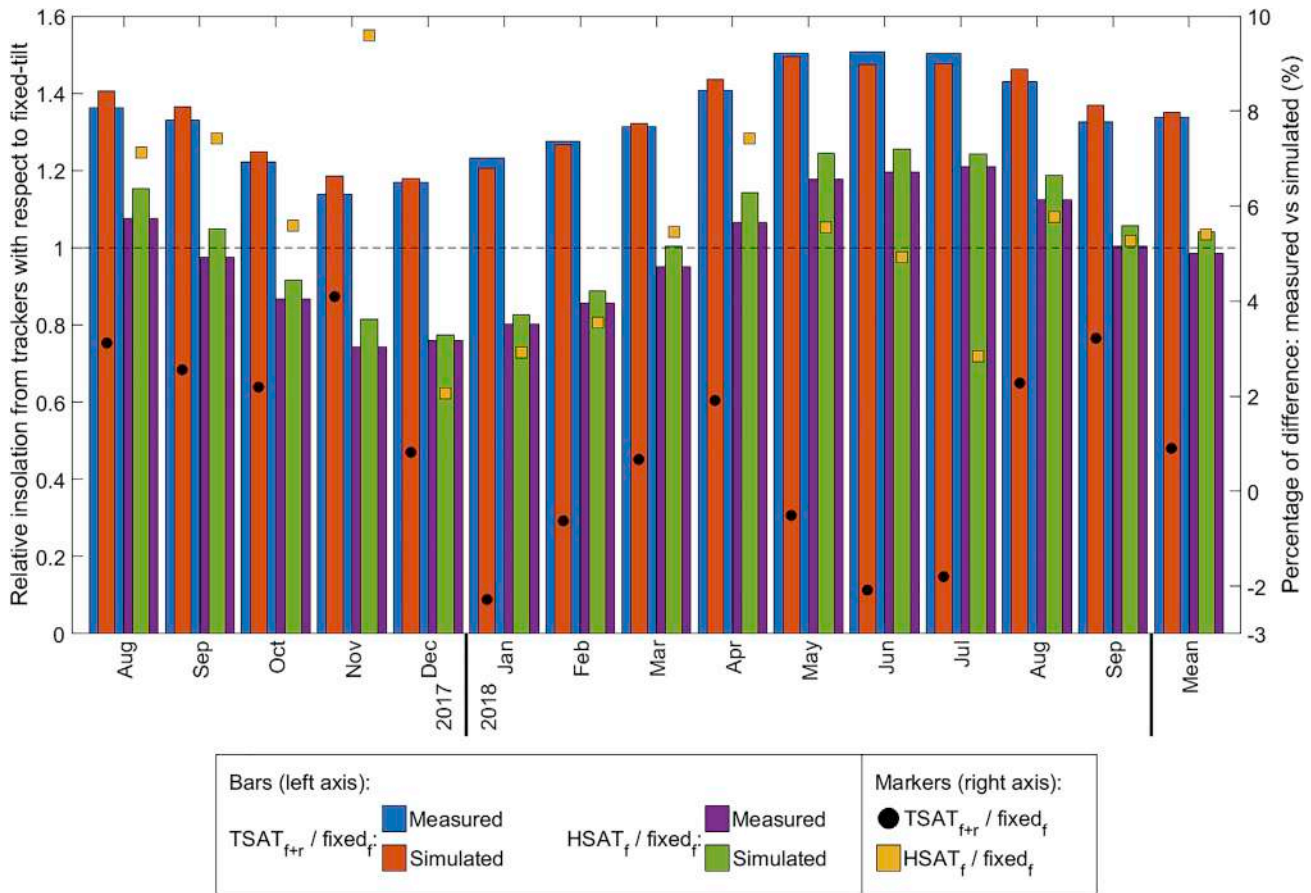


Figure 4. Measured versus Simulated Irradiance Ratios between Tracking and Fixed-Tilt PV Installations Located at China

The bar plots (left y axis) show the measured-based and simulated-based results for the insolation collection ratio between the TSAT (front+rear sides) and HSAT (front side) systems with respect to the fixed-tilt system (front side). The markers show the percentage of difference between the measured and simulated results. The mean values are presented at the last section of this figure.

obtained from the approach used in this paper (also for all sea and land area) is similar: 1.37 and 1.45, respectively. In Pelaez et al.,²¹ bifacial-1T systems reach an average insolation gain of 9% with respect to their monofacial counterparts for many locations worldwide. This is also close to the value of 8% obtained in our work. The small differences are most likely due to the different data sources employed to get the GHI, DNI, and DHI values and the selected models to estimate the front and rear irradiances.

Having validated our method with both real setups and results from the literature, we are confident with our worldwide irradiance estimations employed in the subsequent sections of the paper.

Global Techno-Economic Performance Calculation

To perform the worldwide analysis, other weather parameters besides GHI, DNI, and DHI (discussed in [Calculation of Global/Diffuse Horizontal and Direct Normal Irradiance](#)) are required, such as the daily average ambient temperature and albedo values. These were obtained from CERES for the year 2015,³² which serves as the reference year in this study. This worldwide study features a spatial resolution of 1×1 degrees (for the latitude and longitude), with a 1-h time resolution.

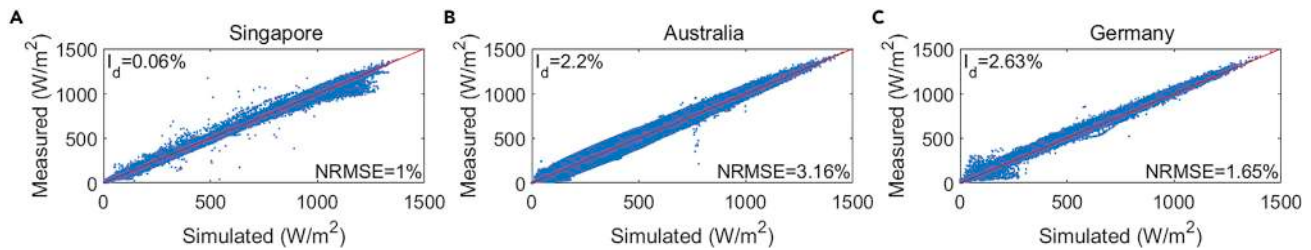


Figure 5. Measured versus Simulated Irradiance Falling at the Front Side of the Modules for the Fixed-Tilt PV Installations Located at Singapore, Australia, and Germany

Validation results for the PV installations located at (A) Singapore, (B) Australia, and (C) Germany. The red line represents the case when measured and simulated values are equal.

In this work, PV farm systems (in the order of the MWp) are assumed. Based on the mounting structure configuration, the monofacial/bifacial module orientation is defined as:

- (1) Fixed-tilt installation: modules have a tilt angle equal to the latitude and are facing the equator. Although this is a typical rule of thumb for monofacial modules, other works have proven that the ideal tilt angle of bifacial modules tends to be higher, e.g., Rodríguez-Gallegos et al.³⁰ Nevertheless, as also shown in Rodríguez-Gallegos et al.,³⁰ the performance improvements are below 4% with an average of 0.6% and therefore, bifacial fixed-tilt modules will use the same tilt as the fixed-tilt installation design for simplicity.
- (2) Single-axis tracker installation (1T): this design can be divided into two subgroups, namely, HSAT and TSAT. Both trackers aim to follow the sun by rotating from east to west with a maximum angle of rotation of $\pm 60^\circ$ (according to datasheets from different manufacturers, e.g., NexTracker,⁴⁹ Soltec,⁵⁰ GameChange Solar,⁵¹ Axisus,⁵² Arctech Solar,⁵³ Nclave,⁵⁴ and Mitbet⁵⁵). Their axis tube is aligned in the north-south line horizontal (for HSAT) and tilted (for TSAT) to ground. For TSAT, a tilt of 30° is selected (as designed by different TSAT manufacturers). The module orientation for HSAT and TSAT are estimated based on Equations 1, 2, 3, and 4 from Marion and Dobos.⁵⁶
- (3) Dual-axis tracker installation (2T): the considered 2T tracker also aims to follow the sun but has two degrees of freedom for its movement. It is assumed that this tracker is able to fully follow the sun during the daytime as many suppliers allow their product to rotate to almost all required orientations.

Furthermore, fixed-tilt modules are considered to be installed with a height of 0.6 m (between their lowest edge and ground), while for the tracking installations, the module middle point is assumed to be 1 m from the ground, and this distance will not vary as the module middle point is assumed to be located at the axis of rotation when dealing with the trackers. Therefore, the front and rear irradiances reaching the module can be calculated for any design, following the approach previously presented in [Energy Generation Modeling](#).

Subsequently, to estimate the energy production from a PV system (see [Energy Generation Modeling](#)), module performance parameters are required. Modules from LONGi Solar have been chosen for this study, as this manufacturer provides both module technologies, thus enabling a fair comparison between monofacial and

Table 2. Parameters of the Selected LONGi Solar Modules

Technology	Monofacial Monocrystalline p-type PERC ⁶⁰	Bifacial Monocrystalline p-type PERC ⁶¹
Module area [m ²]	1.65 × 0.991	1.664 × 0.996
Cost [USD cents/W _p]	26.4	26.4
Module front power under STC [Wp]	310	305
b [%]	N/A	80
γ [%/°C]	−0.37	−0.37
β ₀ [%]	2	2
β ₁ [%/Year]	0.55	0.45
INOCT [°C]	42	42
Power warranty [years]	25	30

bifacial modules. The module characteristics were obtained from datasheets and are presented in Table 2. The module cost was estimated following the approach presented in Kumar et al.,^{57–59}

Table 2 shows that the modules have a power warranty of 25 and 30 years for the monofacial and bifacial technologies, respectively. Therefore, in this work, the system lifetime (l_s) is considered to be 25 years so that all technologies can be compared within the same time range.

Furthermore, similar to Rodríguez-Gallegos et al.,³⁰ the inverter efficiency (η_{inv}) and other related losses (l) are considered to be 96% and 3%, respectively. With the previous data, the energy generation worldwide can then be estimated for different module technologies and installation designs.

With respect to the estimation of the overall system cost (see Estimation of the System Cost), similar to Rodríguez-Gallegos et al.,³⁰ the bank loan is considered to be 60% of the initial investment for all analyzed cases and the debt tenor is assumed to be 10 years. In addition, the bank interest rate is calculated based on the 10-year bond yield of the location of interest,⁶² with a debt premium of 2%. The bank interest rate worldwide is provided in Figure 6A. In addition, the values of the inflation rate⁶³ are presented in Figure 6B. The worldwide discount rate is then calculated based on the previous parameters considering an equity cost estimated from Fernandez et al.⁶⁴ and Damodaran,⁶⁵ and income tax given in Trading Economics;⁶⁶ the estimations are presented in Figure 6C.

Installation cost factor (c_{ins} [USD/Wp]) and O&M factor (c_{OM} [USD/Wp]) of fixed-tilt monofacial monocrystalline p-type passivated emitter and rear cell (PERC) PV systems are calculated with the approach introduced in Rodríguez-Gallegos et al.³⁰ The values of both c_{ins} and c_{OM} can be sub-divided into material and labor costs. The material cost is considered to be identical worldwide, whereas the labor cost is estimated for different countries by taking into account the labor-related costs for Singapore (provided in Rodríguez-Gallegos et al.³⁰) and the relation between the minimum wages in Singapore with respect to the one from all other countries, as shown in Figure 6D (calculated from data provided by Wikipedia⁶⁷).

The four maps presented in Figure 6 show the global distribution of key parameters to calculate the cost of PV systems. These values are provided in Table S1.

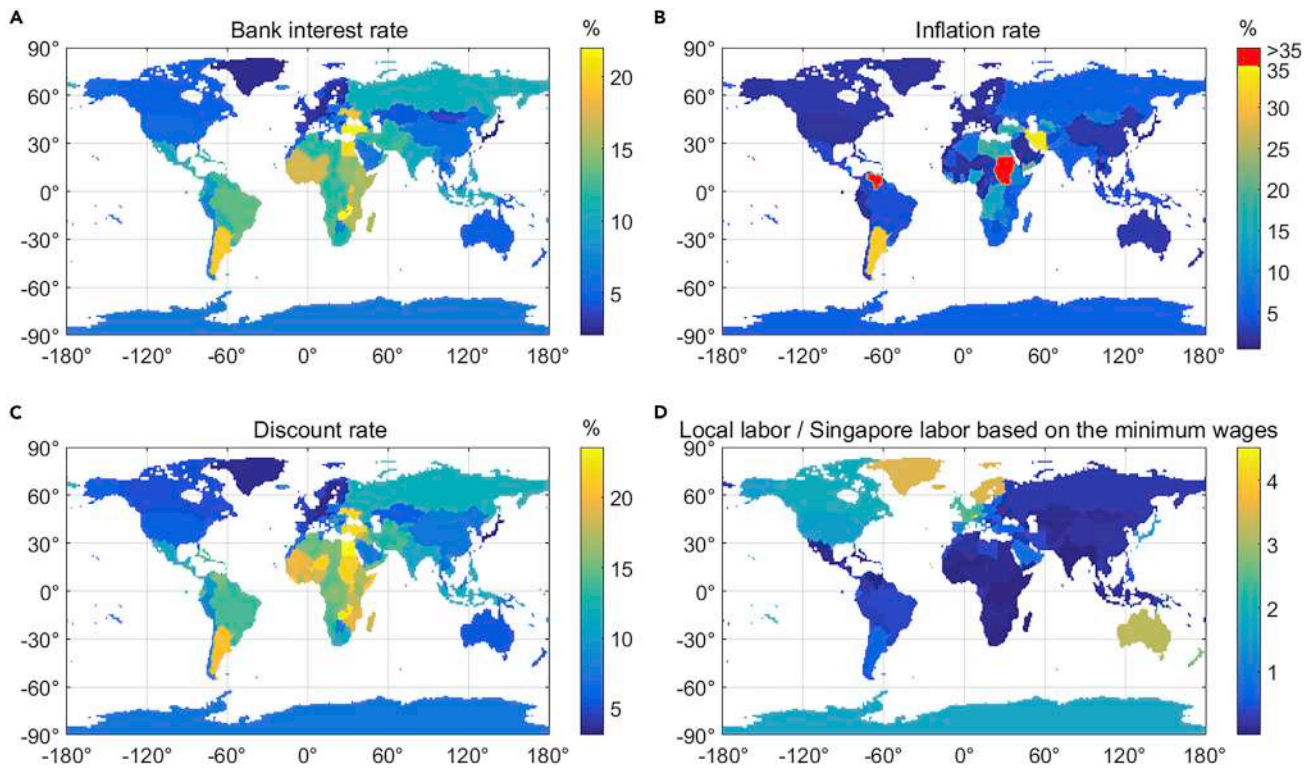


Figure 6. Worldwide Economic Parameters

(A) Bank interest rate, (B) inflation rate (the values for Venezuela, Sudan, and South Sudan are unstable and fall off the charts), (C) discount rate, (D) local labor cost per country relative to the one from Singapore (based on the minimum wages). If any of these values was not available for a particular country, it was estimated based on the nearby countries considering their current economic situation. The values for the Antarctica are rough estimates obtained following the approach from Rodríguez-Gallegos et al., 2017.³⁰ These values are provided as supplementary materials in [Table S1](#).

The estimation of c_{ins} and c_{OM} for the bifacial module technology is obtained considering the relation between its power production and area with respect to the monofacial one (as we consider systems with constant power rating). The mounting structure costs (part of the material cost for c_{ins}) from different manufacturers (including fixed-tilt, single-axis, and dual-axis suppliers) were collected by a comprehensive survey performed by SERIS. The distribution of the collected costs is presented in [Figure 7](#). Median values (0.07 USD/W_p for fixed-tilt, 0.12 for 1T, and 0.40 USD/W_p for 2T systems) are considered in this analysis. Because the obtained costs of the mounting structures for HSAT and TSAT were similar, these were grouped into a single category. Nevertheless, the installation cost for TSAT is expected to be higher due to its foundation requirements, among other factors. However, for simplicity, it will be assumed that this extra cost is minimum. Furthermore, the labor cost when dealing with single- and dual-axis trackers is assumed to be 9% for c_{ins} and 8% for c_{OM} higher than that of fixed-tilt installations.⁹ Note that the analysis in Fu et al.⁹ was performed only for single-axis trackers. Here, we use the same values also for dual-axis trackers.

With respect to PV inverters, investment and warranty costs in the present and for future years are obtained from Rodríguez-Gallegos et al.³⁰ (inverter cost in 2019 is 0.062 USD/W_p). As more power is generated by bifacial modules, it is recommended to increase inverter size by 20%.⁶⁸ Consequently, inverter cost, when dealing with bifacial PV systems, is considered to be 20% higher than for comparable monofacial